FEBS Letters 587 (2013) 833–839

FEBS Letters
journal homepage: www.FEBSLetters.org

Observation of unphosphorylated STAT3 core protein binding to target *ds*DNA by PEMSA and X-ray crystallography

Edwin Nkansah [a], Rahi Shah [a], Gavin W. Collie [a], Gary N. Parkinson [a], Jonathan Palmer [a,2], Khondaker M. Rahman [a,2], Tam T. Bui [b], Alex F. Drake [b], Jarmila Husby [c], Stephen Neidle [c], Giovanna Zinzalla [a,1], David E. Thurston [a,2], Andrew F. Wilderspin [a,*]

[a] *Department of Pharmaceutical and Biological Chemistry, UCL School of Pharmacy, London WC1N 1AX, United Kingdom*
[b] *Biomolecular Spectroscopy Centre, Kings College London, Guy's Campus, London SE1 1UL, United Kingdom*
[c] *CRUK Biomolecular Structure Group, UCL School of Pharmacy, London WC1N 1AX, United Kingdom*

ARTICLE INFO

Article history:
Received 15 November 2012
Revised 17 January 2013
Accepted 24 January 2013
Available online 19 February 2013

Edited by Ivan Sadowski

Keywords:
Signal transducer and activator of transcription 3
STAT3
PEMSA
M67
SH2
X-ray crystallography

ABSTRACT

The STAT3 transcription factor plays a central role in a wide range of cancer types where it is over-expressed. Previously, phosphorylation of this protein was thought to be a prerequisite for direct binding to DNA. However, we have now shown complete binding of a purified unphosphorylated STAT3 (uSTAT3) core directly to M67 DNA, the high affinity STAT3 target DNA sequence, by a protein electrophoretic mobility shift assay (PEMSA). Binding to M67 DNA was inhibited by addition of increasing concentrations of a phosphotyrosyl peptide. X-ray crystallography demonstrates one mode of binding that is similar to that known for the STAT3 core phosphorylated at Y705.

Structured summary of protein interactions:
pSTAT3βtc and **pSTAT3βtc** bind by molecular sieving (View interaction)

1. Introduction

The STAT (signal transducer and activator of transcription) proteins are transcription factors that modulate a number of cellular functions [1]. These proteins can exist as monomers, dimerise to form homodimers, or form heterodimers with other family members [2,3]. STAT3 induces the transcription of genes that control differentiation, inflammation, proliferation, and tumour cell invasion [4,5]. Its over-expression has been implicated in many tumour types [6,7]. According to the original paradigm, cytokines such as interleukin-6 and interferon stimulate the phosphorylation of a specific tyrosine residue of STAT3 (Tyr 705), which confers the ability to sequentially form homodimers that accumulate in the nucleus, and bind to its consensus DNA sequences [2,4,5]. A number of post-translational modifications have also been identified for STAT3, some believed to control dimerisation, others affecting nuclear import/export or DNA binding. Understanding the factors controlling these events, particularly the role of phosphorylation is critical for delineating cell signaling cascades and the development of inhibitors for therapeutic use.

It has been previously reported that phosphorylation is not a pre-requisite for nuclear transport of STAT3, which is dependent on Ran, importin α3 and beta-1 [8,9]. Based on results from a Y705F mutant, a novel mechanism has been suggested whereby unphosphorylated STAT3 (uSTAT3) can have significant transcriptional control over the expression of genes such as RANTES, IL6, IL8, MET and MRAS, which do not respond directly to phosphorylated STAT3 (pSTAT3) [10,11]. Some uSTAT3-responsive genes have kappa B elements, and these genes are activated by a transcription factor complex formed when uSTAT3 binds to unphosphorylated NFκB [11] and not directly to DNA. Some uSTAT3-mediated gene expression is, however, clearly mediated by an NFκB-independent mechanism [11]. Recently, using a 100-fold molar excess, the uS-

Abbreviations: STAT3, signal transducer and activator of transcription 3; SH2, src homology 2 domain; STAT3βtc, the STAT3 core consisting of amino acid residues 127–722; YFP, yellow variant of eGFP, the enhanced green fluorescent protein

* Corresponding author.
E-mail address: a.wilderspin@ucl.ac.uk (A.F. Wilderspin).
[1] Current address: Centre for Advanced Cancer Therapies, MTC, Karolinska Institutet, Nobelsväg 16, 171 77 Stockholm, Sweden.
[2] Current address: Department of Pharmacy, King's College London, Franklin-Wilkins Building, 150 Stamford Street, London SE1 9NH, United Kingdom.

0014-5793/$36.00
http://dx.doi.org/10.1016/j.febslet.2013.01.065

TAT3 core (lacking the N-terminal domain) has been shown to bind directly to a GAS consensus sequence, and also to AT-rich hairpin and cruciform DNA structures by atomic force microscopy [12], furthermore direct binding of the uSTAT1 core protein to its target DNA sequence has been shown [13], where dimerisation was thought to occur at the N-terminal domain. However, quantitative binding of uSTAT3 core directly to DNA has not previously been demonstrated.

Using a novel PEMSA method, we have shown almost quantitative binding of purified uSTAT3 core directly to M67 *ds*DNA, a modified *c-fos* sis inducible enhancer [14], at equimolar concentrations. The unphosphorylated protein:DNA interaction found in the PEMSA studies has been confirmed by X-ray crystallography, and supported by circular dichroism spectroscopy and molecular dynamics simulations. Based on these new data, it can be postulated for the first time that unphosphorylated STAT3 can bind stoichiometrically to a specific enhancer sequence and thereby contribute to the expression of STAT3-dependent genes. STAT1 is known to drive the constitutive expression of several genes through binding DNA without tyrosine phosphorylation [13], and our observations for STAT3 are consistent with this.

2. Methods

2.1. Plasmid construction and expression

The expression construct pYFP-STAT3βtc coding for the fluorescent STAT3βtc fusion protein (Supplementary Information, Fig. S1) was generated by sub-cloning the PCR-amplified eYFP gene into the *Nde*I restriction site at the 5′-end of the STAT3βtc gene. The *Escherichia coli* strain Rosetta was transformed with these constructs to prepare unphosphorylated protein YFP-uSTAT3βtc and uSTAT3βtc, while the strain TKB1 [15] was used to prepare the phosphorylated proteins YFP-pSTAT3βtc and pSTAT3βtc. A 10 L culture was induced when the cells reached exponential phase (A_{600nm} = 0.6) with 1 mM IPTG, and the temperature was reduced from 37 to 21 °C. The culture was harvested by centrifugation 16 h later. To enable phosphorylation, the TKB1 cells were re-suspended in a tryptophan-free media containing indole acrylic acid to induce the plasmid borne Elk kinase, and incubated at 21 °C for 2 h before re-harvesting. A 45 g wet cell pellet was typically obtained for each culture.

2.2. Protein purification

Protein purification was adapted from the method of Becker et al. [16] in which the cells were first lysed by sonication and then centrifuged, but were not treated with PEI (polyethyleneimine) prior to precipitation of the soluble protein (25% w/v ammonium sulphate). Re-suspended protein was purified using HiTrap QFF, and 98% pure STAT3βtc was eluted in 0.1 M NaCl, 100 mM Tris pH 8.5, 1 mM EDTA and 2 mM DTT. YFP-STAT3βtc was eluted in 0.1 M NaCl, 20 mM Hepes pH 7.0, 10 mM $MgCl_2$, 5 mM DTT.

2.3. PEMSA assays

Samples for PEMSA analysis were prepared in PEMSA buffer containing bovine serum albumin (BSA) and sonicated salmon sperm (SSS) to minimise non-specific binding (20 mM Hepes, pH 7.9, 40 mM KCl, 1 mM $MgCl_2$, 0.03 mM EDTA, 0.03 mM EGTA,1 mM DTT, 8% w/v glycerol, 33 μg/ml sonicated salmon sperm, 166 μg/ml BSA). Typically, 3 μg YFP-pSTAT3βtc or YFP-uSTAT3βtc was diluted to a final volume of 15 μl. Double-stranded M67 DNA was prepared by dissolving the two oligonucleotides 5′-TGCATTTCCCGTAAATCT-3′ and 5′-AAGATTTACGGGAAATGC-3′ in 100 mM NaCl at 100 nM each, and annealing from 95 °C for 5 min and slowly cooling to room temperature. For the non-relevant double-stranded control, the annealed DNA sequences were 5′-CTAGCGAAAACTTGTATTTC-CAGGGCG-3′ and 5′-GATCCGCCCTGGAAATACAAGTTTTCG-3′.

Acrylamide PEMSAs were carried out at 150v using 10 × 8 cm 5% native polyacrylamide gels (25 mM Tris, pH 8.2, 22.5 mM Boric acid, 2.5 mM EDTA, 2.5% glycerol) that had been pre-run for 2 h at 4 °C. 10 μl samples were loaded with 8% final concentration of glycerol, but no loading dye. Agarose PEMSAs were carried out at 200v using 15 × 7 cm 2% agarose gels (25 mM Tris, pH 8.2, 22.5 mM Boric acid, 2.5 mM EDTA) at 4 °C. 10 μl samples were loaded with 8% glycerol, and no loading dye.

2.4. Crystallisation

The purified protein was concentrated and buffer exchanged using a 10 kDa centifugal filter (Amicon Ultra) into 20 mM HEPES pH 7.0, 200 mM NaCl, 10 mM $MgCl_2$, 5 mM DTT, 0.5 mM PMSF to a final protein concentration of approximately 5 mg/ml, as determined by UV spectrophotometry (280 nm extinction coefficient = 88 350). A 0.9 mM annealed DNA duplex was obtained by overnight annealing.

Crystallizations used the hanging drop vapour diffusion method. Drops containing 1–2 μl of protein–DNA solution with the same volume of well solution were equilibrated against 500 μl of well solution, incubated at 4 °C, with crystals typically appearing within 48 h. Glycerol was used as a cryoprotectant, in an optimized well solution of 5 mM $MgSO_4$, 10 mM ammonium acetate, 35% glycerol, 50 mM MES pH 6.0 and 300 mM NaCl. Association of duplex DNA with unphosphorylated STAT3βtc resulted in high-quality diffracting crystals.

2.5. Structure solution and refinement

Crystallographic data were collected at the Diamond Light Source on beam line Io4-1, at a wavelength of 0.9785 Å, and 100 K. Processing and data reduction were carried out on site using Xia2, an automated data processing tool within CCP4 [17]. The starting uSTAT3βtc model was derived from pSTAT3βtc (PDB id 1BG1) with all solvent atoms and the phosphorylated tyrosine 705 residue removed. A simple rigid-body refinement was sufficient to initiate refinement, with subsequent refinement and model building cycles performed using Refmac5 [18] and Coot [19]. Data collection and refinement, along with deposition details, are provided in SI Table 1.

2.6. Circular dichroism

All samples were diluted with binding buffer to an optimum measurement concentration of 1.3 μM. The UV absorption and CD spectra were acquired on an Applied Photophysics Chirascan Plus spectrometer (Leatherhead, UK). The spectra were measured in 10 and 0.5 mm rectangular cells in the regions 400–230 and 260–190 nm, respectively. The instrument was flushed continuously with pure evaporated nitrogen throughout the experiments. Spectra were recorded using a 0.5 nm step size, a 1.5 s time-per-point and a spectral bandwidth of 1 nm. The samples were stored in the fridge prior and between repeat measurements. All spectra were buffer baseline subtracted and measured at 25 °C. The CD data were smoothed with a window factor of 4 using the Savitzky–Golay method for presentation purposes (see Supplementary Information for data analysis).

2.7. Molecular dynamics simulations

The model of the pSTAT3βtc:DNA complex was generated by homology modeling, based on a pSTAT3 crystal structure (PDB id

Fig. 1. Schematic representation of the domains and size of the chimeric YFP-STAT3βtc and truncated STAT3βtc core constructs compared to the natural STAT3β.

1BG1 at 2.25 Å resolution). For the uSTAT3βtc:DNA complex version, the phosphoryl-group on Tyr 705 was removed to create a regular Tyr residue. Both of the models included identical 17 bp M67 *ds*DNA with single base overhanging 5′-ends, corresponding to the DNA sequence used in the pSTAT3 experimental study [16].

Both full-atom MD simulations used the GROMACS v 4.5.3 program, employing the improved protein side-chain torsion potentials from the AMBER parm99sb-ILDN force-field, together with the parmbsc0 force-field (a refinement of the AMBER parm99 force field for nucleic acids). Further AMBER parameters for the phosphorylated-Tyr residues were manually ported to GROMACS for the simulations [20]. Further details are provided in the Supplementary Information.

3. Results and discussion

To investigate the STAT3:DNA interaction using PEMSA, we designed a YFP-STAT3βtc construct in which the N-terminal 126 amino acids of STAT3β were replaced with the spectral variants of GFP (Green Fluorescent Protein) from the jellyfish *Aequorea victoria* to act as a reporter (Fig. 1). The STAT3β gene lacks the unstructured C-terminal activation domain present in STAT3α and was used to avoid aggregation of the purified protein [15,21]. The use of the Rosetta strain for expression of uSTAT3 proteins ensured no phosphorylation. Purified samples of phosphorylated YFP-pSTAT3βtc and unphosphorylated YFP-uSTAT3βtc were fractionated by size exclusion chromatography to determine their oligomeric state before addition of DNA. Fig. 2 shows that the purified unphosphorylated protein behaved as a monomer at 16 μM, while the phosphorylated protein had double the molecular weight indicating a dimer. There was very little evidence of higher molecular weight oligomers with this uSTAT3 core, although any large aggregates would have been removed by a 0.22 μm filter before entering the S6 gel filtration column. A small peak at a lower molecular weight was sometimes seen in gel filtration and PEMSA experiments, and was thought to represent a proteolytic product.

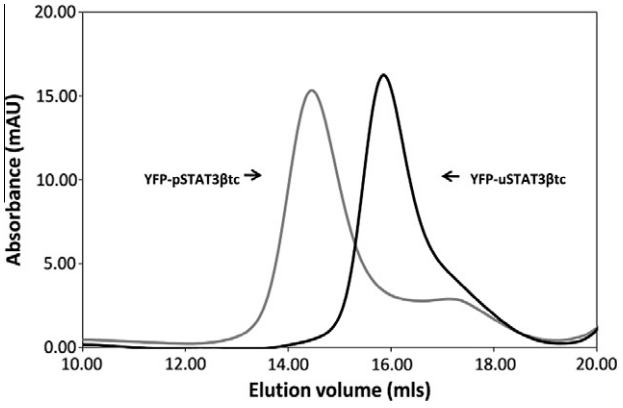

Fig. 2. Size exclusion chromatograms of 160 μg YFP-pSTAT3βtc (dimeric) and YFP-uSTAT3βtc (monomeric) following fractionation (100 μl samples) on a Superose™ 6 (S6) column calibrated with 4 standard protein markers (ovalbumin, 43 kDa; conalbumin, 75 kDa; aldolase, 158 kDa; and thyroglobulin, 669 kDa). The K_{av} values for YFP-pSTAT3βtc and YFP-uSTAT3βtc correlate to 250 and 100 kDa, respectively.

The double-stranded DNA used in the study was M67, a modified c-*fos* sis-inducible enhancer sequence containing the cognate binding site for STAT3. This is the same sequence used in structural studies [16]. Duplex DNA was formed by annealing 5′-TGCATTTCCCGTAAATCT-3′ with a complementary sequence (5′-AAGATTTACGGGAAATGC-3′) containing a 5′-single base overhang. Acrylamide and agarose were investigated for use in the PEMSA experiments and both gave similar results, although agarose PEMSAs were technically easier to perform and afforded a greater distance of separation between free and bound protein. The acrylamide PEMSAs (Fig. 3) allowed faster migration of the protein in the presence of DNA compared to protein alone (lanes 1 *vs* 3–5, and 6 *vs* 9–10). In the absence of SDS in these native gels, the protein charge should be dominant, and so the negative charge of the complex should be significantly greater with DNA-binding leading to faster migration despite increased mass. From the relative migration of the bands in the acrylamide PEMSA, it follows that the unphosphorylated protein (YFP-uSTAT3βtc) alone migrates slightly more slowly than its phosphorylated form (YFP-pSTAT3βtc). The addition of DNA significantly increased the migration distance of both the YFP-uSTAT3βtc and YFP-pSTAT3βtc proteins, clearly indicating that both have a strong interaction with DNA. Observation of a single band (lanes 3–5 and 9–10) indicated complete binding of the full-length fluorescent protein to the DNA. The YFP-pSTAT3βtc:DNA complex ran as a tighter band compared to the YFP-uSTAT3βtc:DNA complex, suggesting a smaller range for the hydrodynamic radius. The titration experiment showed that the transition between free and DNA-bound migration bands (*i.e.*, 50% binding) occurred close to 0.3 μM M67 for phosphorylated STAT3βtc, and close to 0.9 μM M67 for unphosphorylated STAT3βtc. This difference may reflect a different stoichiometry, but could also result from differences in affinity, or a change in the conformation or folding pattern of YFP-uSTAT3βtc compared to YFP-pSTAT3βtc. The PEMSAs were all run with bovine serum albumin and sonicated salmon DNA to minimize non-specific protein/DNA binding, and a further control using the non-relevant double-stranded DNA failed to provide a gel shift (Supplementary Information, Fig. S2).

A Western blot (Supplementary Information, Fig. S3) was performed to further analyze the positions of STAT3βtc in these gels using the K15 antibody. This detected STAT3βtc coincident with the major fluorescent bands, for both free and bound YFP-uSTAT3βtc and YFP-pSTAT3βtc, but did not recognize the faster migrating minor fluorescent bands of constant intensity seen in Figs. 3 and 4, considered to be proteolytic fragments containing YFP. It is noteworthy that YFP has a compact and stable β-barrel arrangement which is known to be more resistant than STAT3 to denaturation and proteolysis, and is therefore likely to persist.

The concentration of uSTAT3 used in PEMSAs (3 μM) was lower than that used in gel filtration (16 μM) where there was no evidence of dimers, so it was initially assumed that the observed YFP-uSTAT3βtc:DNA complex either involved a transient dimeric uSTAT3 core that had dimerized without phosphorylation and which was stabilized in the DNA complex, or otherwise a monomeric uSTAT3 core interacted with DNA without dimerisation. To

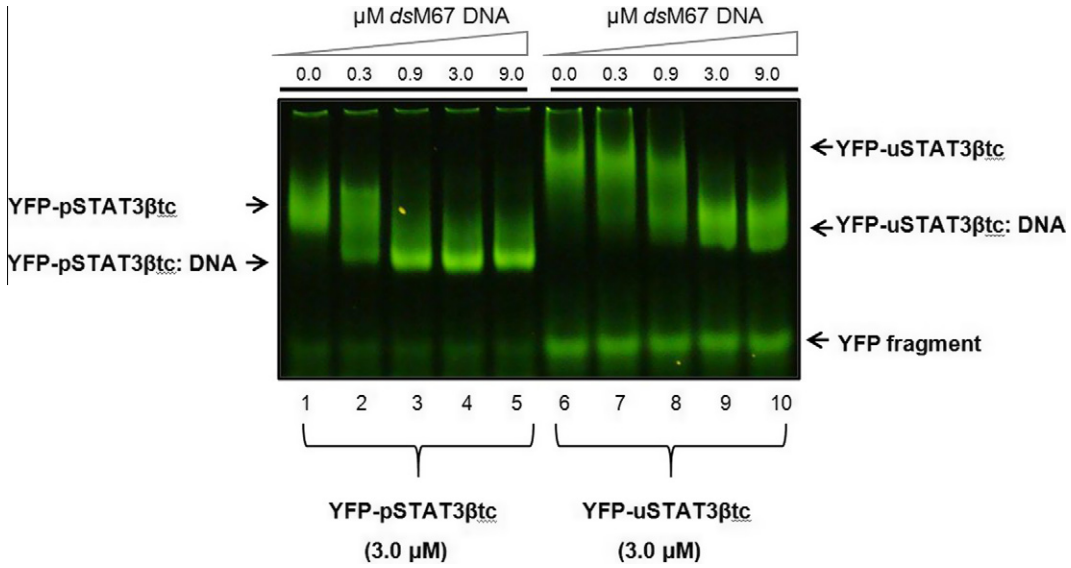

Fig. 3. Polyacrylamide PEMSA showing the relative migration of YFP-uSTAT3βtc and YFP-pSTAT3βtc, and a clear shift for both samples in the presence of M67 DNA containing the cognate recognition sequence. The PEMSA gels were illuminated using a blue light box.

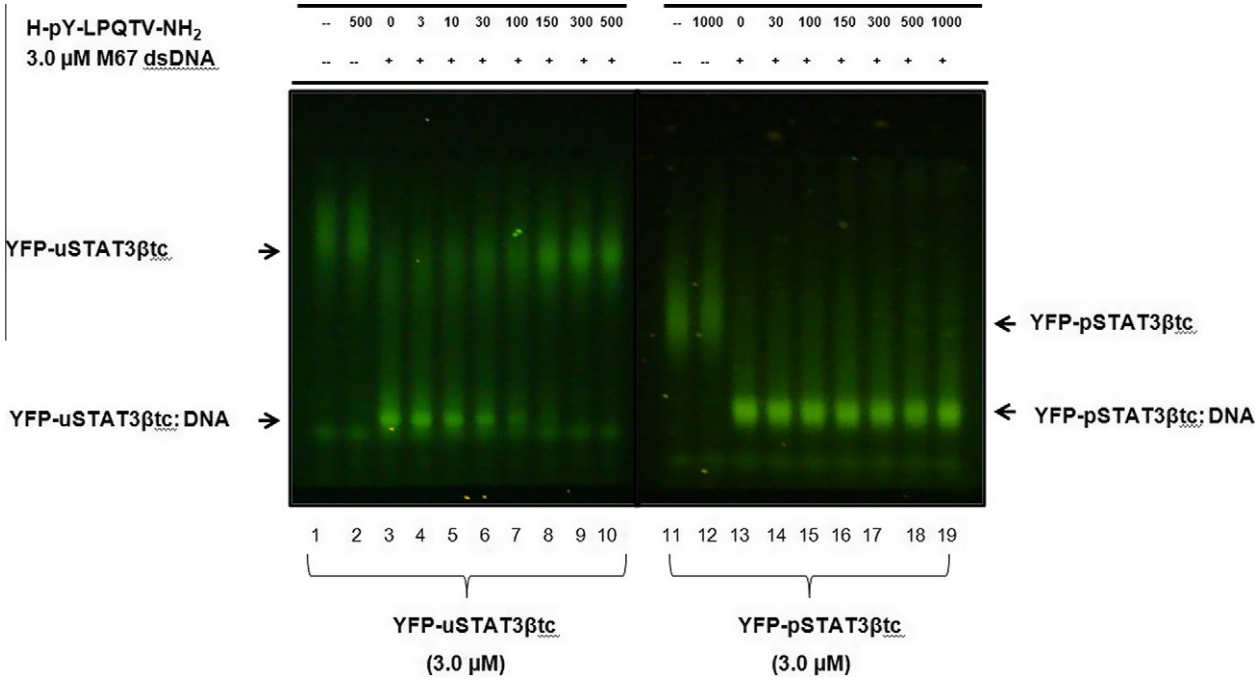

Fig. 4. Agarose PEMSA to show inhibition of DNA binding. YFP-uSTAT3βtc (lanes 3–10) and YFP-pSTAT3βtc (Lanes 13–19) were pre-incubated with M67 *ds*DNA prior to incubation with increasing concentration (μM) of the phosphotyrosyl peptide H_2N-pY-LPQTV-NH_2.

explore this further, a phosphotyrosyl peptide designed to compete for the site occupied by tyrosine 705 at the dimer interface, was introduced to the PEMSA assay in order to evaluate its effect on the YFP-uSTAT3βtc:DNA and YFP-pSTAT3βtc:DNA complexes (Fig. 4). This peptidic sequence, H_2N-pY-LPQTV-NH_2, was derived from the interleukin-6 receptor subunit gp130, and is known to bind to the STAT3 SH2 domain with greater affinity than the homologous peptide H_2N-pY-LKTKFI-NH_2 [22], which was used as a control (Supplementary Information, Fig. S4). We found that H_2N-pY-LPQTV-NH_2 was able to decrease the DNA binding with unphosphorylated STAT3βtc by 50% (DB_{50}) at 30–100 μM, whereas little if any inhibition was observed with phosphorylated STAT3βtc, even at 1000 μM (absolute DB_{50} values are higher than for Ren et al. [22], due to higher substrate concentrations). This result was consistent with disruption of a dimeric uSTAT3 core interaction in the complex, leading to the observed decrease of DNA-binding. The data does not however distinguish whether uSTAT3 cores dimerise before or after binding to DNA.

Crystallographic studies were carried out to further investigate the interactions of uSTAT3 core protein and DNA. Prior to setting-

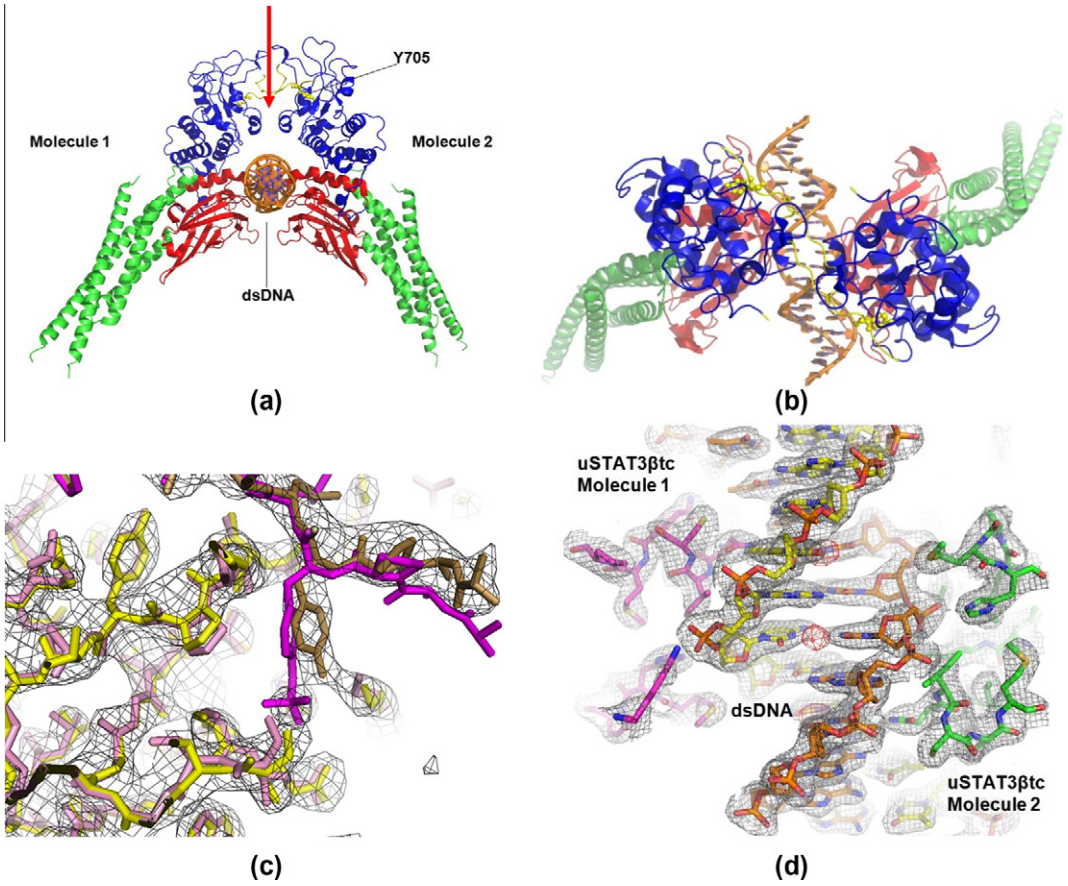

Fig. 5. (a and b) are cartoon representations of uSTAT3βtc:DNA crystal structure (PDB id 4E68). Both panels show two copies of the asymmetric unit. Colour key: green = coiled-coil domain; red = DNA binding domain; blue = SH2 domain; yellow = Y705 linker loop; orange = DNA. Tyrosine 705 is shown as ball-and-stick. The red arrow on panel a indicates the viewing angle for panels b and d. (c) Shows the phosphorylated STAT3βtc structure (1BG1) in purple overlaying the unphosphorylated STAT3βtc structure in gold highlighting the overall realignment of the tyrosine 705 residue. We observe a 2.0 Å displacement of the unphosphorylated tyrosine OH away from the phosphate binding pocket forming a new ion–solvent interaction of distance 3.4 Å. The electron density $2F_o–F_c$, is drawn at the 1σ level. (d) Reveals the uSTAT3β3tc:DNA interface in detail. The $2F_o–F_c$, electron density map (grey) and $F_o–F_c$ residual density map (red) highlight the quality of the refined structure and accuracy of the atomic coordinate data.

up crystallizations, the buffer-exchanged uSTAT3βtc protein was mixed with equimolar annealed DNA duplex (0.9 mM stock solution) at 4 °C and incubated for 30 min, allowing formation of the uSTAT3βtc:DNA complex. The same duplex oligonucleotide (M67) as used in the PEMSA experiments was selected for these crystallization studies, as it contains the modified nine base-pair consensus sequence to which pSTAT3βtc dimers are known to bind with higher affinity [16].

A crystal structure of the uSTAT3βtc:DNA complex was determined and refined to 2.6 Å. This structure displays an isomorphous mode of protein:DNA binding as seen in the equivalent phosphorylated structure (PDB id 1BG1) [16], which involves two molecules of uSTAT3βtc binding to the duplex DNA via their DNA-binding domains in a symmetric dimeric arrangement (Fig. 5a and b). This uSTAT3βtc:DNA crystal structure therefore provides evidence in support of the hypothesis that, under certain conditions, unphosphorylated STAT3 is able to bind to a target DNA sequence as a dimer. Structural alignment of the uSTAT3βtc:DNA crystal structure and the previously determined pSTAT3βtc:DNA crystal structure (PDB id 1BG1) reveals very little difference between these complexes (RMSD = 0.66 Å for 558 C_α atoms). Realignment of the unphosphorylated tyrosine can be seen in Fig. 5c, and the ends of the alpha helices connecting the missing loop residues 184–194 are slightly more ordered. All other parts of the structures are essentially unchanged. Fig. 5d clearly shows electron density for the DNA and DNA-interacting residues of the protein. Residual density appearing between the DNA bases represents un-modelled duplex DNA since the space group selection imposes a twofold equivalence. Coordinates and structure factors are available from the PDB (PDB id 4E68). A structural alignment with the monomeric

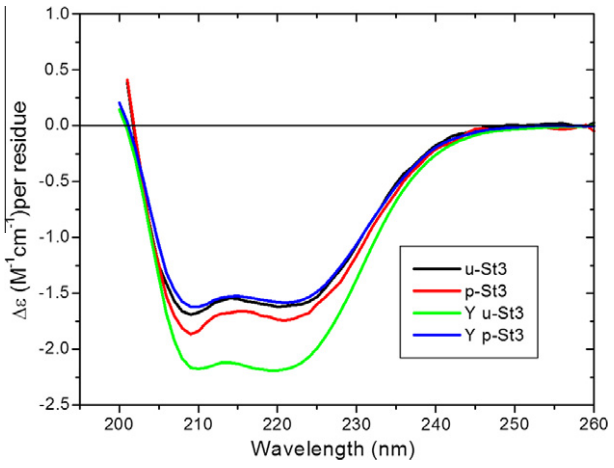

Fig. 6. Far-UV CD spectra of YFP-tagged STAT3βtc (Y u-St3 and Y p-St3) and untagged STAT3βtc (u-St3 and p-St3) proteins.

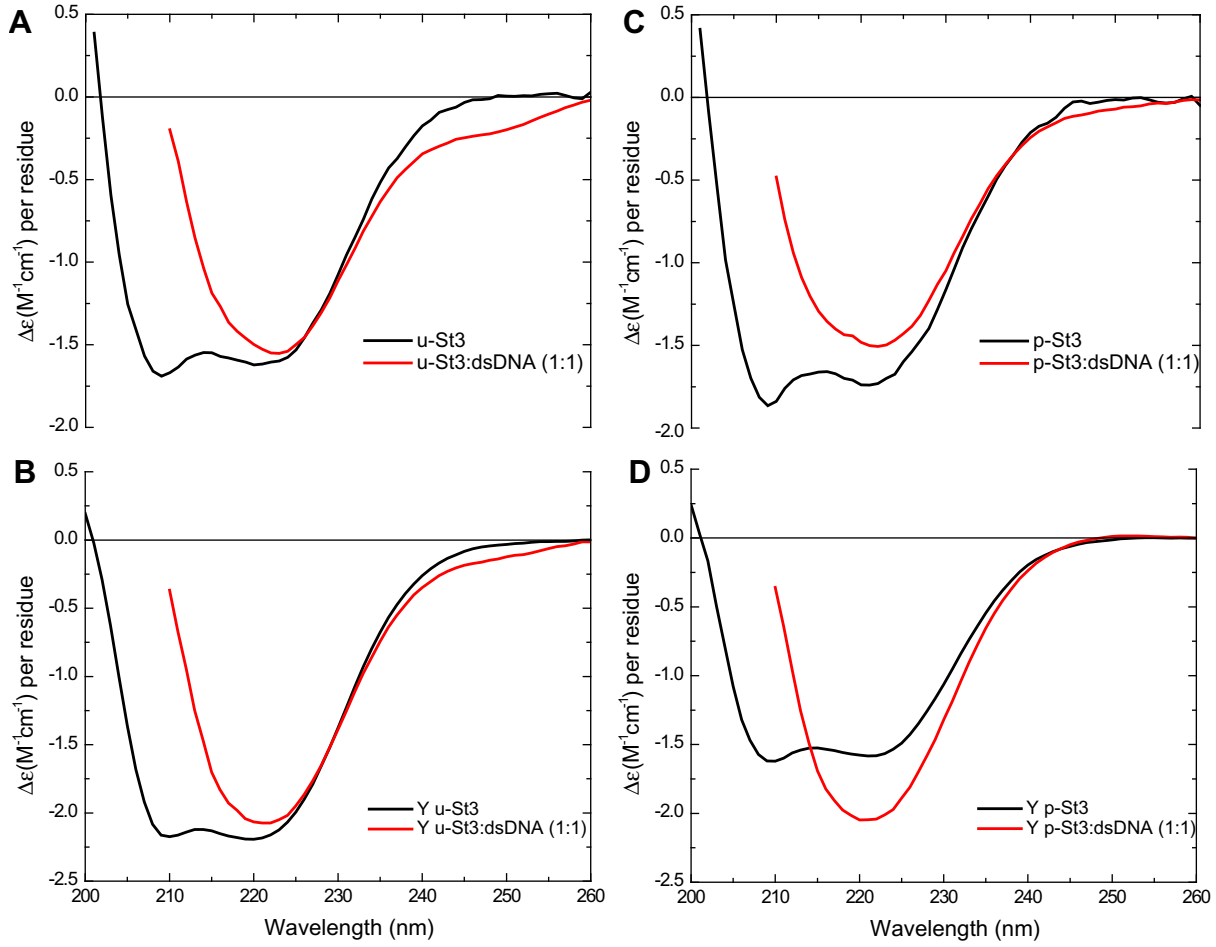

Fig. 7. CD spectra of STAT3 proteins alone and in association with M67 dsDNA after subtraction of dsDNA alone. (A) uSTAT3βtc; (B) YFP-uSTAT3βtc; (C) pSTAT3βtc; (D) YFP-pSTAT3βtc.

STAT3 crystal structure that lacks the phosphotyrosine region (residues 689–722) and is free from DNA (PDB id 3CWG) [23] reveals only a slightly greater difference (RMSD = 0.95 Å for 500 C_α atoms).

Circular dichroism spectroscopy was used to provide information about any possible folding effect of the YFP tag on DNA binding. Tagged and untagged uSTAT3 and pSTAT3 proteins were studied, and the CD spectra in the far-UV region suggested that all four were well-folded and adopted stable conformations (Fig. 6). However, incubating the STAT3 proteins with 1 equiv of the M67 *ds*DNA and recording the CD spectra after 5 min provided significant changes confirming the association with *ds*DNA (Fig. 7). A change in secondary structure was immediately obvious after association with the DNA (see calculation of secondary structure components in Supplementary Information). In each case, a small decrease in α-helix component was observed with a corresponding increase in β-sheet component.

A molecular dynamics simulation was carried out with the uSTAT3 monomer and uSTAT3 dimer in complex with M67 DNA to obtain further information about the roles of the different uSTAT3 structures in association with their cognate DNA sequence. Molecular modelling and full atomistic molecular dynamics (MD) simulations were employed to systematically evaluate the binding free energy for the association of both the phosphorylated (pSTAT3βtc) and unphosphorylated (uSTAT3βtc) STAT3βtc:DNA complexes. Based on the MD ensemble structures, the interaction energies and solvation free energies over the course of a 30 ns trajectory (1200 snapshots with 25 ps time-steps) were calculated by means of the MM-PBSA (molecular mechanics (MM) Poisson Boltzmann/Generalized Born surface area MM-GBSA) approach implemented in AMBER 11, for STAT3:STAT3 association, as well as for STAT3:DNA association. The calculated binding free energy (ΔG_{bind}) for the STAT3:STAT3 interaction in the pSTAT3βtc complex was −194.8 kcal/mol using the MMPBSA method, and −174.6 kcal/mol using the MMGBSA method, while values of −95.2 kcal/mol (MMPBSA) and −96.4 kcal/mol (MMGBSA), respectively, were obtained for the uSTAT3 protein–protein interaction. Hence, the binding free energy of the protein–protein association was calculated to be approximately twofold more favourable for pSTAT3βtc than for the uSTAT3βtc complex. For the protein–DNA association, the calculated binding energies (ΔG_{bind} values; MMPBSA and MMGBSA methods) were −137.1 and −88.2 kcal/mol for the pSTAT3βtc:DNA complex, and −140.1 and −89.8 kcal/mol for the uSTAT3βtc:DNA complex. These energies were in good qualitative agreement with the experimental data described above.

4. Conclusion

We have demonstrated by PEMSA that unphosphorylated STAT3 protein can bind almost quantitatively to M67 *ds*DNA. X-ray crystallographic studies showed that the interaction with DNA is very similar to that of phosphorylated STAT3. These observations have been further supported by CD spectroscopy and

molecular dynamics simulations. The proposed mechanism for transcriptional control of STAT3-dependent genes has generally been based on the concept that phosphorylation of uSTAT3 is a prerequisite for DNA binding and transcriptional activation. The results reported here substantially support the hypothesis that uSTAT3 as well as pSTAT3 can bind directly to DNA in order to play a role in gene regulation. In the oncology area, all STAT3 drug discovery research to date has focused on inhibitors targeted to the phosphorylated STAT3 protein [24–26], and although to date there have been no reports of the targeting of uSTAT3 by small molecules for therapeutic purposes, Stark and co-workers [10,11,27] have reported potential roles of uSTAT3 in oncogenesis and signalling in cancer cells. Therefore, the results reported here support their findings and suggest that uSTAT3 could be a novel drug target in oncology.

Acknowledgements

Cancer Research UK is acknowledged for supporting this work (C180/A9327 to D.E.T., and C129/A4489 to S.N.). The Ghana Education Trust Fund is also acknowledged for a studentship (to EN). Dr. C. Muller is thanked for providing the STAT3β plasmid, and we are grateful to the Diamond Light Source for access to Beamline ID I04-1. We are grateful to Applied Photophysics Ltd (Surrey, UK) for providing the Chirascan™ instrument (to A.D.), and to the Wellcome Trust for supporting the KCL Biomolecular Spectroscopy Centre.

Appendix A. Supplementary data

Supplementary data associated with this article can be found, in the online version, at http://dx.doi.org/10.1016/j.febslet.2013.01.065.

References

[1] Bromberg, J. and Darnell, J.E. (2000) The role of STATs in transcriptional control and their impact on cellular function. Oncogene 19, 2468–2473.
[2] Leonard, W.J. and O'Shea, J.J. (1998) Jaks and STATS: biological implications. Annu. Rev. Immunol. 16, 293–322.
[3] Levy, D.E. and Darnell, J.E. (2002) STATs: transcriptional control and biological impact. Nat. Rev. Mol. Cell Biol. 3, 651–662.
[4] Zhong, Z., Wen, Z.L. and Darnell, J.E. (1994) STAT3 – a STAT family member activated by tyrosine phosphorylation in response to epidermal growth-factor and interleukin-6. Science 264, 95–98.
[5] Darnell, J.E. (1997) STATs and gene regulation. Science 277, 1630–1635.
[6] Nakajima, K. et al. (1996) A central role for Stat3 in IL-6-induced regulation of growth and differentiation in M1 leukemia cells. EMBO J. 15, 3651–3658.
[7] Bowman, T., Garcia, R., Turkson, J. and Jove, R. (2000) STATs in oncogenesis. Oncogene 19, 2474–2488.
[8] Liu, L., McBride, K.M. and Reich, N.C. (2005) STAT3 nuclear import is independent of tyrosine phosphorylation and mediated by importin-alpha 3. Proc. Nat. Acad. Sci. USA 102, 8150–8155.
[9] Cimica, V., Chen, H.-C., Iyer, J.K. and Reich, N.C. (2011) Dynamics of the STAT3 transcription factor: nuclear import dependent on Ran and importin-beta1. PLoS One 6, e20188.
[10] Yang, J., Chatterjee-Kishore, M., Staugaitis, S.M., Nguyen, H., Schlessinger, K., Levy, D.E. and Stark, G.R. (2005) Novel roles of unphosphorylated STAT3 in oncogenesis and transcriptional regulation. Cancer Res. 65, 939–947.
[11] Yang, J., Liao, X., Agarwal, M.K., Barnes, L., Auron, P.E. and Stark, G.R. (2007) Unphosphorylated STAT3 accumulates in response to IL-6 and activates transcription by binding to NF{kappa}B. Genes Dev. 21, 1396–1408.
[12] Timofeeva, O.A. et al. (2012) Mechanisms of unphosphorylated STAT3 transcription factor binding to DNA. J. Biol. Chem. 287, 14192–14200.
[13] Chatterjee-Kishore, M., Wright, K.L., Ting, J.P.Y. and Stark, G.R. (2000) How Stat1 mediates constitutive gene expression: a complex of unphosphorylated Stat1 and IRF1 supports transcription of the LMP2 gene (vol. 19, pp. 4111, 2000). EMBO J. 19, 4855.
[14] Yang, E., Lerner, L., Besser, D. and Darnell, J.E. (2003) Independent and cooperative activation of chromosomal *c-fos* promoter by STAT3. J. Biol. Chem. 278, 15794–15799.
[15] Becker, S., Corthals, G.L., Aebersold, R., Groner, B. and Muller, C.W. (1998) Expression of a tyrosine phosphorylated, DNA binding Stat3 beta dimer in bacteria. FEBS Lett. 441, 141–147.
[16] Becker, S., Groner, B. and Muller, C.W. (1998) Three-dimensional structure of the Stat3 beta homodimer bound to DNA. Nature 394, 145–151.
[17] Winn, M.D. et al. (2011) Overview of the CCP4 suite and current developments. Acta Crystallogr., Sect. D 67, 235–242.
[18] Murshudov, G.N., Vagin, A.A. and Dodson, E.J. (1997) Refinement of macromolecular structures by the maximum-likelihood method. Acta Crystallogr., Sect. D 53, 240–255.
[19] Emsley, P. and Cowtan, K. (2004) Coot: model-building tools for molecular graphics. Acta Crystallogr., Sect. D 60, 2126–2132.
[20] Husby, J., Todd, A.K., Haider, S.M., Zinzalla, G., Thurston, D.E. and Neidle, S. (2012) Molecular dynamics studies of the STAT3 homodimer:DNA complex: relationships between STAT3 mutations and protein–DNA recognition. J. Chem. Inf. Model. 52, 1179–1192.
[21] Vinkemeier, U., Cohen, S.L., Moarefi, I., Chait, B.T., Kuriyan, J. and Darnell, J.E. (1996) DNA binding of in vitro activated Stat1 alpha, Stat1 beta and truncated Stat1: interaction between NH2-terminal domains stabilizes binding of two dimers to tandem DNA sites. EMBO J. 15, 5616–5626.
[22] Ren, Z.Y., Cabell, L.A., Schaefer, T.S. and McMurray, J.S. (2003) Identification of a high-affinity phosphopeptide inhibitor of Stat3. Bioorg. Med. Chem. Lett. 13, 633–636.
[23] Ren, Z.Y. et al. (2008) Crystal structure of unphosphorylated STAT3 core fragment. Biochem. Biophys. Res. Commun. 374, 1–5.
[24] Johnston, P.A. and Grandis, J.R. (2011) STAT3 signaling: anticancer strategies and challenges. Mol. Interv. 11, 18–26.
[25] Page, B.D.G., Ball, D.P. and Gunning, P.T. (2011) Signal transducer and activator of transcription 3 inhibitors: a patent review. Expert Opin. Ther. Pat. 21, 65–83.
[26] Yue, P. and Turkson, J. (2009) Targeting STAT3 in cancer: how successful are we? Expert Opin. Investig. Drugs 18, 45–56.
[27] Yang, J.B. and Stark, G.R. (2008) Roles of unphosphorylated STATs in signaling. Cell Res. 18, 443–451.